Hybrid Asymmetrical Load Modulated Balanced Amplifier With Wide Bandwidth and Three-Way-Doherty Efficiency Enhancement

Yuchen Cao, *Graduate Student Member, IEEE*, and Kenle Chen, *Member, IEEE*

***Abstract*— This letter presents a new active-load-modulation power amplifier (PA) architecture, i.e., hybrid asymmetrical load modulated balanced amplifier (H-ALMBA). It is discovered that the control amplifier (CA) of load modulated balanced amplifier (LMBA) can be set as the carrier amplifier and the balanced amplifier (BA) as the peaking amplifier with different threshold settings for two subamplifiers, BA1 and BA2. Through proper amplitude and phase control and cooperative alignment of the turning-on sequence of BA1 and BA2, the entire H-ALMBA can achieve enhanced efficiency overextended power back-off range, similar to a three-way Doherty PA. More importantly, this hybrid load modulation behavior can be replicated over a nearly unlimited frequency span. The theory is well validated by a prototype developed using GaN technology and commercial quadrature couplers, which experimentally demonstrates a 4:1 RF bandwidth from 0.55 to 2.2 GHz and high efficiency, i.e., 55%–82% at peak power, 51%–69% at 5-dB power back-off and 40%–61% at 10-dB power back-off.**

***Index Terms*— Balanced amplifier (BA), Doherty, high efficiency, high-peak-to-average power ratio (PAPR), load modulation (LM), power amplifier (PA), wideband.**

I. Introduction

WIDEBAND and complex waveforms are increasingly utilized in advanced radars [1] and communication systems, e.g., 5G and WiFi6 [2]. Besides the significantly enhanced system capabilities and spectral efficiency, these modulated signals can have very large variations of the instantaneous envelope, quantified as peak-to-average power ratio (PAPR). Amplifying such signals using conventional high-power amplifiers (HPAs) is subject to unforgiving degradation of efficiency. As a result, enhancing power amplifier (PA) efficiency at power back-off is of crucial importance for realizing energy-efficient radar and communication systems.

Supply modulation, i.e., envelope tracking (ET) and load modulation (LM) are two major technological solutions for PA back-off efficiency enhancement. ET suffers from limited modulation bandwidth and requires an extra supply modulator [3], which prohibits its applications in array-based systems, e.g., massive multi-in–multi-out (MIMO) and active electronically scanned array (AESA). Circumventing these issues, LM exhibits promising potential for realizing next-generation high-efficiency PAs [4]. However, the most widely employed LM architecture, Doherty PA (DPA), is intrinsically narrowband. Despite recent advances, the development of wideband DPA with meanwhile large dynamic power range is still very challenging. Moreover, to accommodate the ever-increasing PAPR of signals, high-order LM (e.g., three-way DPA [5]) becomes necessary to enhance the efficiency between two peaks at saturation and the target back-off level (normally equal to PAPR) [6].

To address these issues, a novel LM architecture, i.e., hybrid asymmetrical load modulated balanced amplifier (H-ALMBA), is presented in this letter. Derived from the recently proposed asymmetrical load modulated balanced amplifier (ALMBA) [7], [8], the design space of load modulated balanced amplifier (LMBA) is substantially extended by incorporating an advanced Doherty biasing scheme into the circuitry, which engenders a new hybrid LM mode similar to a three-way DPA. Not only is this H-ALMBA endowed with the intrinsic wideband capability of symmetrical LMBA, but it also achieves enhanced efficiency across the entire power range down to >10-dB back-off, as demonstrated by measurements.

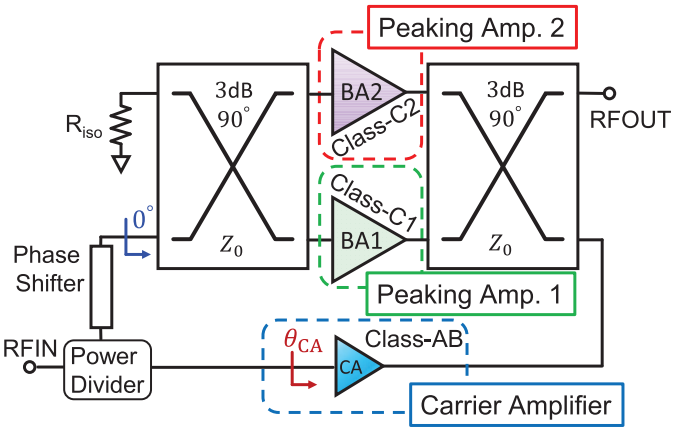

Fig. 1. General schematic of RF-input hybrid asymmetrical LMBA.

II. Hybrid Asymmetrical LMBA

Developed from the reported pseudo-Doherty LMBA (PD-LMBA) [7], the proposed H-ALMBA is analyzed in this section. As described in Fig. 1, the H-ALMBA consists of a balanced amplifier (BA) and a control amplifier (CA) [8],

Manuscript received March 11, 2021; accepted March 16, 2021. Date of publication March 24, 2021; date of current version June 7, 2021. This work was supported by the National Science Foundation under Award 1914875. *(Corresponding author: Kenle Chen.)*

The authors are with the Department of Electrical and Computer Engineering, University of Central Florida, Orlando, FL 32816 USA (e-mail: yuchencao@knights.ucf.edu; kenle.chen@ucf.edu).

This article was presented at the IEEE MTT-S International Microwave Symposium (IMS 2021), Atlanta, GA, USA, June 6–11, 2021.

Color versions of one or more figures in this letter are available at https://doi.org/10.1109/LMWC.2021.3068613.

Digital Object Identifier 10.1109/LMWC.2021.3068613

the LM behaviors of BA1, BA2, and CA can be expressed as

$$Z_{b1} = Z_0\left(\frac{I_{b2}}{I_{b1}} + \frac{\sqrt{2}I_c e^{j\theta}}{I_{b1}}\right)$$
$$Z_{b2} = Z_0\left(2 - \frac{I_{b1}}{I_{b2}} + \frac{\sqrt{2}I_c e^{j\theta}}{I_{b2}}\right)$$
$$Z_c = Z_0\left(1 - \sqrt{2}\frac{I_{b1} - I_{b2}}{I_c e^{j\theta}}\right) \quad (1)$$

where I_{b1}, I_{b2}, and I_c are the magnitude of BA1, BA2, and CA currents, respectively, and θ is the phase of the control path. It can be seen from (1) that by offsetting the symmetry of I_{b1} and I_{b2}, the LM of three individual amplifiers can be controlled concurrently. Further, if BA1 and BA2 are turned on sequentially at different power levels, a hybrid LM mode can be achieved.

A. Hybrid Asymmetrical LMBA Theory

As depicted in Fig. 1, the CA is set as the carrier amplifier, while BA1 and BA2 are biased as peaking amplifiers with different thresholds. As the input power increases, the operation of H-ALMBA can be mainly divided into the following three regions.

1) *Low-Power Region ($P_{OUT} < P_{Max}$/LBO):* In this region, the BA is turned off, i.e., $I_{b1,2} = 0$. The impedances of BA1 and BA2 are thus equal to ∞, and the output power is completely generated by the CA so that the overall H-ALMBA efficiency is equal to the CA efficiency. The load impedance of CA is constantly equal to Z_0 within this region. When the output power reaches the target low-back-off (LBO) level, CA is designed to reach saturation for maximum back-off efficiency.
2) *Doherty Region (P_{Max}/LBO$\leq P_{OUT} \leq P_{Max}$/HBO):* With output power higher than LBO level, the BA1 is turned on and I_{b1} starts to increase, while BA2 remains off. According to (1), the CA is load modulated with the increase of I_{b1} similar to the carrier amplifier of DPA, and I_c continues to increase, shown in Fig. 2. Until the power reaches high-back-off (HBO) level, CA and BA1 can be seen as a two-way Doherty-like amplifier.
3) *ALMBA Region (P_{Max}/HBO $\leq P_{OUT} \leq P_{Max}$):* As the power further increases, BA2 is turned on. I_{b2} starts to increase sharply, while I_{b1} continues to grow. It is noted that I_{b2} raises at a larger slope than I_{b1} until they both reach the same maximum at P_{Max}. In this region, as shown in Fig. 2, the CA LM moves backward with slightly degraded I_{CA} due to the steeper increase of I_{b2}. This effect does not affect the overall power and efficiency, as the power generation is dominated by BA in this region.

B. Amplitude and Phase Control

To achieve maximized efficiency at power back-off, CA needs to be saturated at target HBO which can be achieved properly setting $V_{DD,CA}$ and $R_{OPT,CA}$. At the same time, BA1 and BA2 need to be turned on at the target LBO and HBO, respectively, which can be achieved by setting the power dividing ratio between BA and CA and properly choosing threshold voltages of BA1 and BA2 [9].

It can be calculated from (1) that the LM trajectories of CA, BA1, and BA2 are primarily determined by the phase of the CA (θ_{ca}). Ideally, this phase offset needs to be 0° in order to route the desired LM trajectories on real axis. In realistic design, the phase control can be conducted by properly setting the length of delay lines at the input of BA and CA [10].

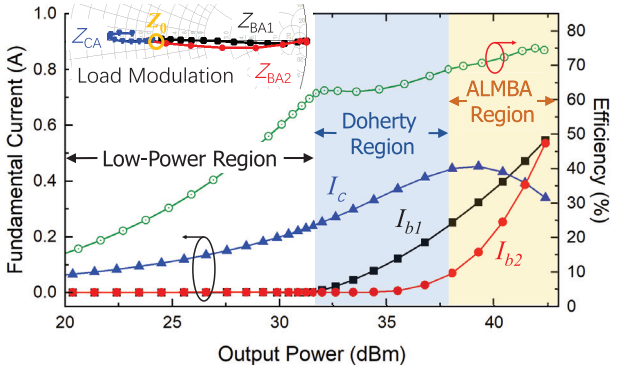

Fig. 2. Simulated fundamental currents versus output power of BA1, BA2, and CA; the drain efficiency changes at three power regions and load-modulation trajectories (inset Smith chart).

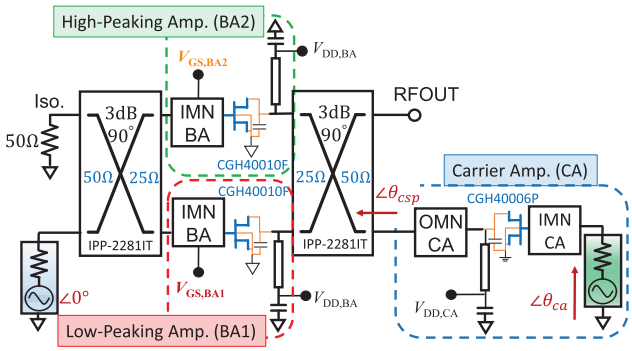

Fig. 3. Realistic design of the proposed H-ALMBA using wideband impedance-transformer coupler and GaN transistors (dual-input is for analysis only and will be merged to RF-input in the final implementation).

III. Design of Ultrawideband H-ALMBA

Following the proposed H-ALMBA theory and the ideal schematic in Fig. 1, the physical circuits of the CA and BA are built using 6-W GaN device (Wolfspeed CGH40006P) and 10-W GaN devices (Wolfspeed CGH40010F), respectively. The realized circuit schematic is shown in Fig. 3. The target LBO and HBO levels are set to 10 and 5 dB, respectively, and the frequency range is targeted from 0.55 to 2.2 GHz.

A. BA and CA Design

Similar to [7], [8], two impedance transformers (2:1) couplers (IPP-2281IT) are used to combine BA1 and BA2 in the quadrature phase. The output impedance matching of BA1 and BA2 is realized using the impedance transformer coupler and the bias lines, leading to reduce the broadband phase dispersion that normally occurs in complex matching networks [11] and eased phase equalization of BA and CA.

The broadband impedance design of CA must take into account both the stand-alone efficiency at low-power region and the phase equalization with BA1 and BA2 in the LM regions. Therefore, the output matching of CA finally adopts the multisegment transmission-line matching method, which leads to linear phase-frequency dependence and eases the phase control as compared to the low-pass network [12].

B. Phase Shifter Design and Reciprocal Biasing for Wideband H-ALMBA

The phase shifter design of H-ALMBA is similar to [7], [8], [10], since the optimal phase control in theory is

TABLE I
STATE-OF-THE-ART OF WIDEBAND LOAD-MODULATED PAS

Ref. / Year	Architecture	Freq. (GHz)	FBW (%)	P_{Max} (dBm)	DE @ P_{Max} (%)	DE @ HBO (%)	DE @ LBO (%)
[13] 2017	RF-Input LMBA	1.8-3.8	71	44	46-70	30-53@5 dB*	20-25@10 dB*†
[14] 2018	Dual-Input LMBA	1.7-2.5	38	48-48.9	48-58*	38-46@5 dB*	33-45@10 dB*†
[15] 2019	3-Way DPA	1.6-2.6	48	45.5-46	53-66	47-57@5 dB*	50-53@9.5 dB
[16] 2019	DEPA	2.55-3.8	40	48.8-49.8	54-67	42.5-57.5@5 dB*	47-60@8 dB
[17] 2020	CM-LMBA	1.45-2.45	52	45.6-46.7	67.1-77.9	46-55@5 dB*	37-43@10 dB*
This Work	H-ALMBA	0.55-2.2	120	41-43	55-82	51-69@5 dB	40-61@10 dB

* Graphically estimated, † PAE.

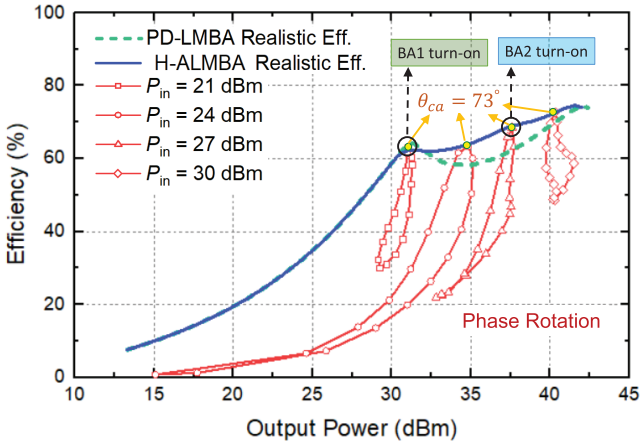

Fig. 4. Phase and amplitude control of H-ALMBA at 1.0 GHz.

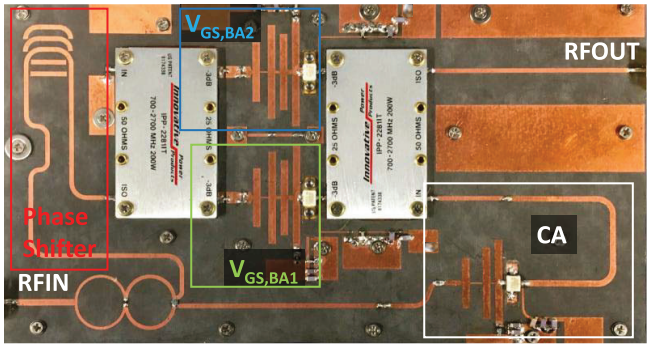

Fig. 5. Fabricated H-ALMBA prototype.

the same as the symmetrical LMBA. Fig. 4 shows the simulated efficiency profile of the realistic H-ALMBA at 1 GHz, in which the optimal control phase of CA is determined by sweeping the input phase. Repeating this process at different frequencies reveals that the optimal phase offset is linearly proportional to frequency, and thus, a transmission line can be placed at CA input to provide the wideband phase control. For ideal H-ALMBA operation, BA1 turns on earlier than BA2, which is valid only for ideal quadrature coupler. To overcome the frequency-dependent imperfections of a realistic coupler, the turning-on sequence of BA1 and BA2 can be interchanged at different frequencies, leading to a wideband H-ALMBA.

IV. IMPLEMENTATION AND EXPERIMENTAL RESULTS

To validate the proposed method, a prototype is developed and fabricated on Rogers 5880 substrate, as shown in Fig. 5. The BA is implemented using two Wolfspeed

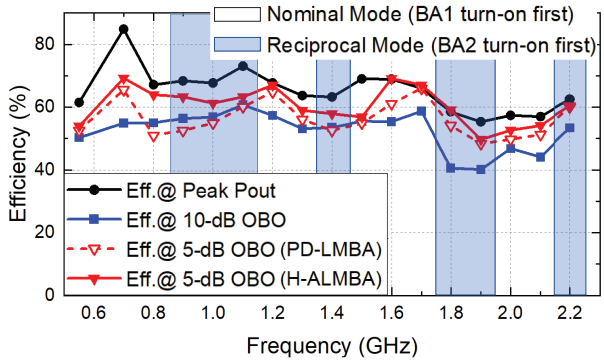

Fig. 6. Measured efficiency various OBO levels from 0.55 to 2.2 GHz.

CGH40010 devices biased in Class-C mode with a V_{DD} of 28 V, and the output matching is provided by the transformer (50 Ω/25 Ω) coupler. The CA is implemented using CGH40006, and it is biased in Class-AB with a $V_{\mathrm{DD,CA}}$ of 11 V, which ensures its saturation at 10-dB power back-off.

The prototype is measured with a continuous-wave (CW) stimulus signal. As shown in Fig. 6, a dual-octave bandwidth of LM is achieved from 0.55 to 2.2 GHz. An efficiency of 55%–82% is measured at peak power, 51%–69% at 5-dB output power back-off (OBO), 40%–61% at 10-dB OBO. Compared to the symmetrical PD-LMBA (dashed line in red) [7], the efficiency within the target OBO is significantly enhanced (solid line in red). The measured performance compares favorably with the state-of-the-art, as summarized in Table I.

V. CONCLUSION

A novel active-LM PA architecture, hybrid asymmetrical LMBA, is introduced for the first time. By properly setting different turning-on thresholds of BA1 and BA2 together with desired phase and amplitude controls from CA, a hybrid LM behavior can be achieved close to a three-way DPA. With this unique cooperation of CA and BA, the H-ALMBA not only offers enhanced efficiency across extended dynamic power range but also fully inherits the wideband feature from the conventional symmetrical LMBA. To experimentally validate the proposed theory, a wideband H-ALMBA prototype is designed and implemented. Measurement results show that the developed H-ALMBA exhibits highly efficient performance over a 4 : 1 bandwidth. Across this frequency span, specifically, it delivers >60% of efficiency at peak power while achieving >40% efficiency at all back-off levels down to 10-dB OBO. The H-ALMBA significantly expands the design space of quadrature-coupler-based LM platform, showing promising potential for applications in future multiband wireless communication systems.

REFERENCES

[1] Z. Dunn, M. Yeary, C. Fulton, and R. Rincon, "Impedance-dependent wideband digital predistortion of solid-state radar amplifiers," *IEEE Trans. Aerosp. Electron. Syst.*, vol. 53, no. 5, pp. 2290–2303, Oct. 2017.

[2] E. G. Larsson, O. Edfors, F. Tufvesson, and T. L. Marzetta, "Massive MIMO for next generation wireless systems," *IEEE Commun. Mag.*, vol. 52, no. 2, pp. 186–195, Feb. 2014.

[3] B. Kim *et al.*, "Push the envelope: Design concepts for envelope-tracking power amplifiers," *IEEE Microw. Mag.*, vol. 14, no. 3, pp. 68–81, May 2013.

[4] S. Hu, F. Wang, and H. Wang, "A 28-/37-/39-GHz linear Doherty power amplifier in silicon for 5G applications," *IEEE J. Solid-State Circuits*, vol. 54, no. 6, pp. 1586–1599, Jun. 2019.

[5] S. Chen, W. Wang, K. Xu, and G. Wang, "A reactance compensated three-device Doherty power amplifier for bandwidth and back-off range extension," *Wireless Commun. Mobile Comput.*, vol. 2018, pp. 1–10, Jan. 2018.

[6] H. Lyu, Y. Cao, and K. Chen, "Linearity-enhanced quasi-balanced Doherty power amplifier with mismatch resilience through series/parallel reconfiguration for massive MIMO," *IEEE Trans. Microw. Theory Techn.*, early access, Feb. 15, 2021, doi: 10.1109/TMTT.2021.3056488.

[7] Y. Cao and K. Chen, "Dual-octave-bandwidth RF-input pseudo-Doherty load modulated balanced amplifier with $\geq$ 10-dB power back-off range," in *IEEE MTT-S Int. Microw. Symp. Dig.*, Aug. 2020, pp. 703–706.

[8] Y. Cao, H. Lyu, and K. Chen, "Asymmetrical load modulated balanced amplifier with continuum of modulation ratio and dual-octave bandwidth," *IEEE Trans. Microw. Theory Techn.*, vol. 69, no. 1, pp. 682–696, Jan. 2021.

[9] Y. Cao, H. Lyu, and K. Chen, "Load modulated balanced amplifier with reconfigurable phase control for extended dynamic range," in *IEEE MTT-S Int. Microw. Symp. Dig.*, Jun. 2019, pp. 1335–1338.

[10] Y. Cao and K. Chen, "Pseudo-Doherty load-modulated balanced amplifier with wide bandwidth and extended power back-off range," *IEEE Trans. Microw. Theory Techn.*, vol. 68, no. 7, pp. 3172–3183, Jul. 2020.

[11] D. J. Shepphard, J. Powell, and S. C. Cripps, "An efficient broadband reconfigurable power amplifier using active load modulation," *IEEE Microw. Wireless Compon. Lett.*, vol. 26, no. 6, pp. 443–445, Jun. 2016.

[12] K. Chen and D. Peroulis, "Design of highly efficient broadband class-E power amplifier using synthesized low-pass matching networks," *IEEE Trans. Microw. Theory Techn.*, vol. 59, no. 12, pp. 3162–3173, Dec. 2011.

[13] P. H. Pednekar, E. Berry, and T. W. Barton, "RF-input load modulated balanced amplifier with octave bandwidth," *IEEE Trans. Microw. Theory Techn.*, vol. 65, no. 12, pp. 5181–5191, Dec. 2017.

[14] R. Quaglia and S. Cripps, "A load modulated balanced amplifier for telecom applications," *IEEE Trans. Microw. Theory Techn.*, vol. 66, no. 3, pp. 1328–1338, Mar. 2018.

[15] J. Xia, W. Chen, F. Meng, C. Yu, and X. Zhu, "Improved three-stage Doherty amplifier design with impedance compensation in load combiner for broadband applications," *IEEE Trans. Microw. Theory Techn.*, vol. 67, no. 2, pp. 778–786, Feb. 2019.

[16] P. Saad, R. Hou, R. Hellberg, and B. Berglund, "An 80W power amplifier with 50% efficiency at 8dB power back-off over 2.6-3.8 GHz," in *IEEE MTT-S Int. Microw. Symp. Dig.*, Jun. 2019, pp. 1328–1330.

[17] J. Pang, C. Chu, Y. Li, and A. Zhu, "Broadband RF-input continuous-mode load-modulated balanced power amplifier with input phase adjustment," *IEEE Trans. Microw. Theory Techn.*, vol. 68, no. 10, pp. 4466–4478, Oct. 2020.